Haze Measurements through Image Analysis

by

Nilu Zhao

B.S., Mechanical Engineering (2014)

Massachusetts Institute of Technology

Submitted to the Department of Mechanical Engineering
In Partial Fulfillment of the Requirements for the Degree of
Bachelor of Science in Mechanical Engineering

at the

Massachusetts Institute of Technology

June 2014

Signature redacted

Signature of Author... ....
Department of Mechanical Engineering
May 11, 2014

Certified by.. Signature redacted ....
George Barbastathis
Professor of Mechanical Engineering
Thesis Supervisor

Signature redacted

Accepted by..... ....
Anette Hosoi
Associate Department Head for Education/ Professor
Undergraduate Officer

Haze Measurements through Image Analysis

by

Nilu Zhao

Submitted to the Department of Mechanical Engineering
on May 9, 2014 in Partial Fulfillment of the
requirements for the Degree of Bachelor of Science in
Mechanical Engineering

ABSTRACT

In the recent years, Singapore has been affected by haze caused by slash-and-burn fires in Indonesia. Currently, haze concentration is measured by filtering air samples at various stations in Singapore. In this thesis, optical approaches to haze measurements are explored. Images of haze were taken in fifteen minute intervals in June, 2013. These images were analyzed to obtain image contrast, and power spectral density functions. The power spectral density functions were characterized by maximum power, full width at half maximum, second and third moments, and exponential fit. Out of these methods, contrast and exponential fit results showed trend to the Pollutant Standards Index (PSI) values provided by the National Environmental Agency (NEA). Further studies on mapping contrast to PSI values are recommended.

Thesis Supervisor: George Barbastathis

Title: Professor of Mechanical Engineering

Acknowledgements

The author would like to thank Professor Barbastathis for his help, support, and guidance in this project. The author would like to thank Wensheng Chen for his help and discussions in this project; Zhi Chen and Yubo Duan for their help in setting up the experiment; Hosea Siu for providing comments and editing this thesis.

Table of Contents

1. Introduction

1.1 What is Haze?

Haze is an environmental occurrence in which the air in the atmosphere is filled with dust, smoke and small particles. Haze is different from smog in that the former is caused by dust small particles present in the air, while the latter is caused by the presence of the combination of smoke and fog.

Haze occurrences in the Southeast Asian region dates back as early as the 1980s. In recent years, haze occurrences in Southeast Asia were caused by slash-and-burn agricultural practices, in which trees are cut and burnt to provide fertility to soil.

1.2 Haze in Singapore in 2013

The level of hazardousness of air is measured in PSI, the Pollutant Standards Index. The higher the value of PSI, the more polluted the air. In June and July of 2013, Singapore was hit by highest haze levels in 16 years("Singapore, Malaysia Hit by Haze" 2014). Singapore experienced high PSI levels of haze where the air was very hazardous for the body. The haze was caused by land and forest fires in Sumatra, an island in Indonesia. Many fires occurred in the eastern areas of central Sumatra, which is to the southwest of Singapore. The haze from the fires was blown over to Singapore due to the wind coming from southeast and southwest directions during Southwest Monsoon season, which is experienced by Southeast Asia regions between June and October of that year (World Meteorological Organization 2013). Figure 1 shows an example of the haze in Singapore in June 2013. Figure 2 shows the direction of wind in Southeast Asia region on June 20th 2013.

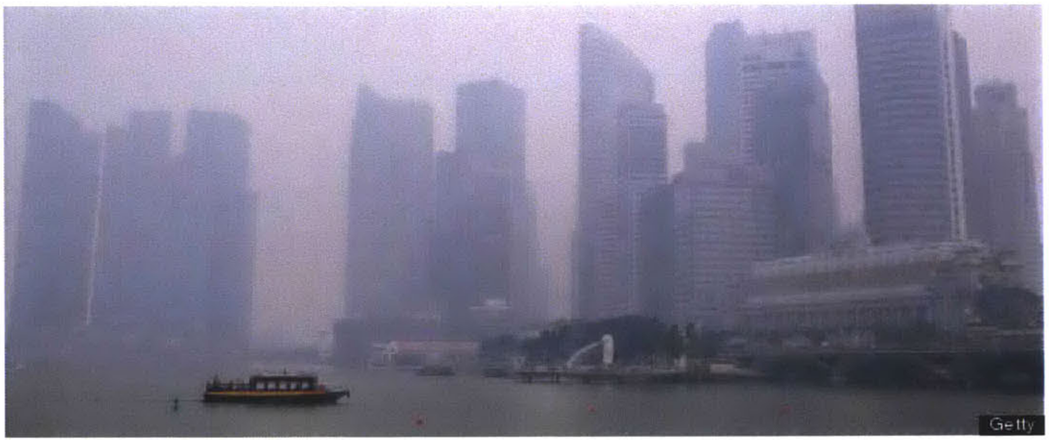

Figure 1. Picture of Singapore on June 20th 2013 (Chris McGrath/Getty Images, 2013).

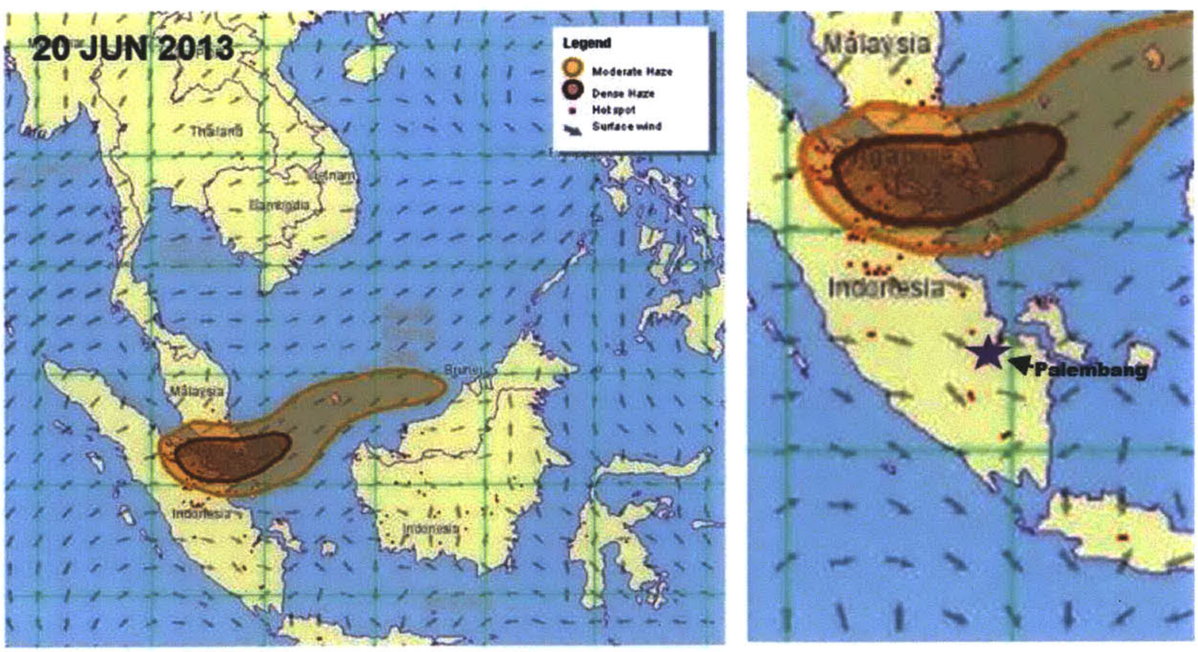

Figure 2. Regional haze map for June 20th 2013. Arrows indicate wind directionality, light brown indicates area of moderate haze PSI level, dark brown indicates area of dense haze of high PSI level, and red dots indicate hot spots where there were fires ("Meteorological Service Singapore" 2013)

1.3 Haze Composition and Health Effects

Haze is composed of smoke, dust, and small particles including particulate matter and sulfur dioxide, carbon monoxide, and nitrogen dioxide. Particulate matter is a mixture of small particles and droplets that contain acids, metals, and soil particles (US EPA 2014). These particles enter the lungs and can cause serious health effects including nose and eyes irritation. Long exposure to haze can lead to chronic heart and lung disease ("NEA Spells Out How PSI Is Compiled" 2014)

1.4 Current Methods of Haze Measurement

PSI measurements give an indication of how hazardous air quality is to human health. Table 1 shows the air quality correspondence to PSI.

Table 1. Correspondence between PSI and air quality. Note that the Singapore National Environment Agency uses this table to classify air quality for 24 hr averages, not 3 hr averages of PSI.

PSI Value	PSI Descriptor
0-50	Good
51-100	Moderate
101-200	Unhealthy
201-300	Very Unhealthy
Above 300	Hazardous

PSI is computed by measuring the concentration of six pollutants: particulate matter (PM_{10}), fine particulate matter ($PM_{2.5}$), sulfur dioxide (SO_2), carbon monoxide (CO), ozone (O_3) and nitrogen dioxide (NO_2). The concentration of each pollutant is then converted to a sub-index by linearly calibrating the concentration to the segment of the scale that the concentration falls in. The scale extends from 0 to 500. The overall PSI is the maximum of the sub-indices (Singapore NEA Computation). Table 2 below shows the breakpoints of the scale for each pollutant.

Table 2. Breakpoints used in defining pollutant sub-indices. When 8 hour ozone concentration exceeds 785 micrograms per cubic meter, the PSI sub-index is calculated suing the 1 hour concentration. (Singapore NEA)

Index Category	PSI	24-hr $PM_{2.5}$ ($\mu g/m^3$)	24-hr PM_{10} ($\mu g/m^3$)	24-hr SO_2 ($\mu g/m^3$)	8-hr CO (mg/m^3)	8-hr O_3 ($\mu g/m^3$)	1-hr NO_2 ($\mu g/m^3$)^
Good	**0 – 50**	0 – 12	0 – 50	0 – 80	0 – 5.0	0 – 118	-
Moderate	**51 – 100**	13 – 55	51 – 150	81 – 365	5.1 – 10.0	119 – 157	-
Unhealthy	**101 – 200**	56 – 150	151 – 350	366 – 800	10.1 – 17.0	158 – 235	1130
Very Unhealthy	**201 – 300**	151 – 250	351 – 420	801 – 1600	17.1 – 34.0	236 – 785*	1131 – 2260
Hazardous	**301 – 400**	251 – 350	421 – 500	1601 – 2100	34.1 – 46.0	786 – 980*	2261 – 3000
	401 – 500	351– 500	501 – 600	2101 – 2620	46.1 – 57.5	981 – 1180*	3001– 3750

The haze condition in Singapore in 2013 was the worst since 1997, reaching PSI reading to as high as 401 PSI for 3 hour averages.

1.5 Current Measurement Equipment and Methods

Singapore has 14 networked stations across the country to monitor and analyze air quality to provide particulate matter concentration values. To obtain these concentrations, each station draws air samples into a chamber where particulate matter sticks to a filter. Then a beta ray is passed through the filter and based on the resulting intensity of the ray the amount of particulate matter can be measured ("NEA Spells Out How PSI Is Compiled" 2014). The sample air is passed through many filters of different pore sizes to determine the concentration of 2.5 micro particles ($PM_{2.5}$), and 10 micron particles (PM_{10}). The data is then transmitted by each station in the network to a Central Control System to be processed so that the Central Control System can publish real time updates. The stations are checked regularly to ensure that the equipment are maintained and operated properly. In 2003 alone, 644 equipment inspections were conducted, and 42 failed to comply with standards. In the same year, the NEA received 480 complaints relating to air pollution, and the main causes were due to poor machine maintenance, improper operation, and overloading of pollution control equipment ("Country Synthesis Report on Urban Air Quality Management" 2006).

Figure 3. Haze monitor station at NEA ("How Does Singapore Measure Haze Levels?" 2014).

1.6 Background

In the past, optical research has been conducted on haze and the atmosphere. E. O. Hulburt looked into the magnitude of the attenuation of light in haze and fog, and the angular distribution of light scattered by haze. Hulburt's results showed pronounced forward scattering of light by haze (Hulburt 1941). E. J. McCartney investigated atmospheric scattering and examined the structure and composition of the gas atmosphere, taking kinetic theory, atmospheric envelope, and quantitative treatments of optical paths into account (McCartney 1976). In another related paper, G. W Kattawar and G. N. Plass, calculated the scattering matrix for a typical haze and cloud from the Mie theory (Kattawar and Plass 1968). Many studies of turbulence used optical methods. Phase contrast imaging is a technique that is applied in a number of such studies (Lin et al. 2009). Power spectral density is a tool that is used in obtaining surface topography and light scattering (Duparré et al. 2002).

More recently, researchers in Singapore used optical approaches to examine PSI values. They studied the spatial and temporal variability of haze, and focused on areas without ground-based instrumentations. Moderate Resolution Imaging Spectroradiometer (MODIS) on satellites was used to obtain imagery of the haze. The imagery allowed them to derive the columnar aerosol optical thickness (AOT). Correlations between measurements of AOT and PM_{10} measurements were conducted, and the results showed that the MODIS AOT had similar trends to the actual PSI values and that MODIS AOT can be used to estimate air quality categories defined by the PSI (Chew et al. 2009)

1.7 Motivation

The NEA publishes haze measurements on three- and twenty-four hour intervals, releasing to the public the average values of haze measurements in the last three hours and last day respectively during 2013. Starting from April 2014, the NEA subsumed $PM_{2.5}$ data into PSI, and started reporting hourly updates. Current means of measuring haze level are complicated. As mentioned in Section 1.5, the station equipment needs to be checked periodically, samples can only be drawn from where those stations are, and readings are updated only hourly. Optical approaches are promising: they are faster than current methods, and are simple to set up. Optical methods give the possibility of obtaining haze information at many more locations and in a more frequent manner. The motivation behind this thesis is to conduct a study into optical methods of measuring haze that are faster and simpler than current means.

2. Experiment

2.1 Experiment Configuration

Taking images of the hazy air was the starting point of this investigation. A digital SLR Canon camera was set up on the 10^{th} floor sky garden of the CREATE building at National University of Singapore. Images were captured in 15-minute intervals from the afternoon of June 20th 2013, until the afternoon of June 24th 2013. Figure 4 shows the experiment setup.

2.2 Field of view

The field of view was fixed for convenience of image comparison. The camera focused on an observable landmark, the SingTel Microwave Tower. The distance between the CREATE Tower (1 Create Way) and the SingTel Microwave Tower (1010 Dover Rd) is approximately 0.64km. Figure 5 shows an image taken by the camera. The images were taken in Canon Raw image file. The CR2 files were then converted to TIFF format to preserve all the information in the image, with 5616 pixels by 3744 pixels at 96 dpi.

Figure 4. The experiment setup consisted of a digital SLR Canon camera setup on the 10th floor on the CREATE building at NUS and a computer which programmed the camera to capture images.

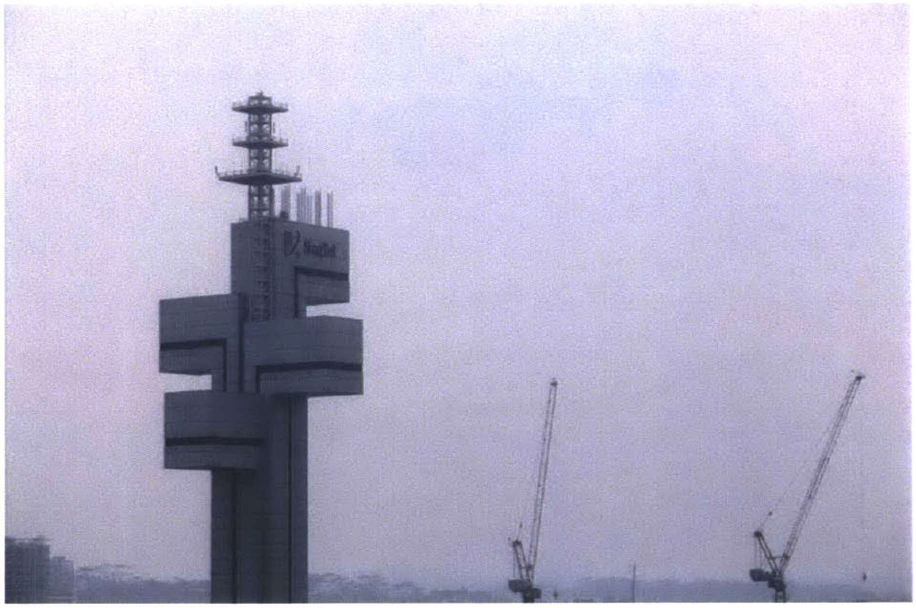

Figure 5. Image of the atmosphere and the SingTel tower on June 24th 2014 at 12pm.

2.3 Data

The Sigapore NEA took PSI measurements of both PM_{10} and $PM_{2.5}$. (Before April 1st 2014, $PM_{2.5}$ concentration was not included into its 3 hour PSI readngs.)

Table 3 shows the 3 hour PSI readings from June 17th to June 24th.

Table 3. 3 hour PSI readings from June 17th to June 24th, 2014 (NEA)

	June 20th	June 21st	June 22nd	June 23rd	June 24th
12am	218	210	180	91	76
1am	195	173	183	90	70
2am	N/A	143	180	88	64
3am	N/A	119	179	89	59
4am	N/A	104	177	93	54
5am	N/A	96	180	99	51
6am	137	94	190	104	48
7am	128	111	231	106	47
8am	122	158	292	105	47
9am	131	256	323	101	47
10am	153	367	326	96	49
11am	198	400	322	90	52
12pm	299	401	319	83	54
1pm	371	360	263	80	59
2pm	355	245	178	78	65

3pm	312	168	122	78	72
4pm	253	145	85	77	79
5pm	268	143	73	77	82
6pm	310	139	73	76	79
7pm	292	135	77	75	75
8pm	231	137	82	75	72
9pm	197	142	87	76	68
10pm	231	153	90	79	65
11pm	250	168	91	80	61

3. Methods and Results

Several image analysis methods were conducted on the images to find correlations between PSI and the images. These methods include image contrast, and several analyses and characterization of the power spectral density. Out of the many methods, contrast was shown to be the most effective in relating the images to the official PSI readings.

3.1 Contrast Method

3.1.1 Luminance

Luminance measures the luminous intensity in a given direction per area. Captured images were imported and read in MATLAB, where each image pixel was captured in RGB values, and for each image, these values were recorded in a 3744x5616x3 matrix. To obtain the luminance of the images, the MATLAB function rgb2gray was used, which calculates perceived luminance by weighing each of the RGB values that accounts for human perception. The equation is given below,

$$I = 0.2989R + 0.5870G + 0.1140B, \qquad \text{Eq. (1)}$$

where I denotes luminance, and R, G, and B denote red, green, and blue values respectively. This method from MATLAB function rgb2gray eliminates the hue and saturation information, while retaining the luminance. The 3D matrices were thus converted into 2D matrices that contained the luminance information.

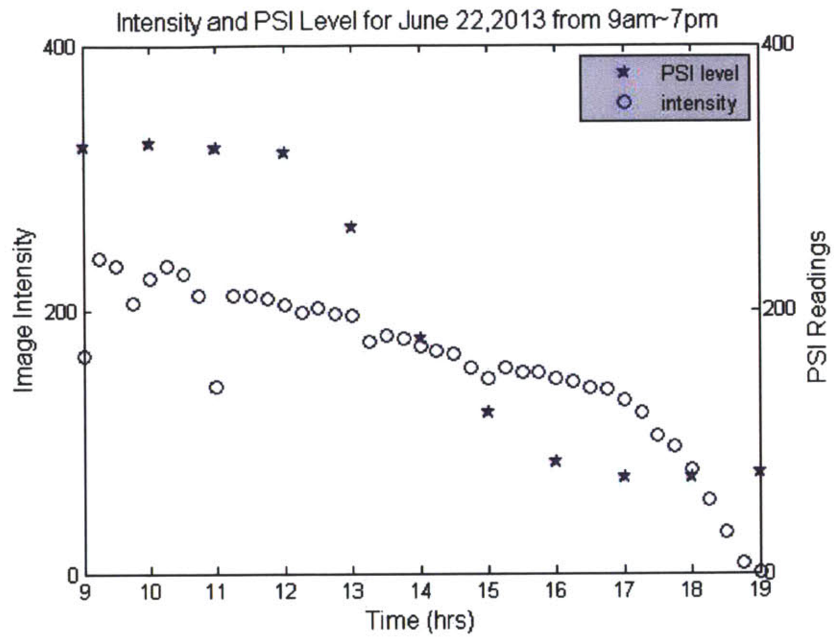

3.1.2 Contrast

Contrast is the difference in luminance in an image that makes its features distinguishable. There are many definitions of contrast, including the Weber contrast, the Michelson contrast, and RMS contrast. The Weber contrast is often used for small features, when the average luminance is approximately the background luminance. The Michelson contrast is commonly used when bright and dark features take up similar amount of area. The root mean squared contrast is defined as the standard deviation of pixel intensities. The Michelson contrast equation was used in calculating contrast because of the grid like pattern which is the focus of contrast in this particular patch of image. The Michelson contrast equation, is as follows

$$Contrast = \frac{I_{\max} - I_{\min}}{I_{\max} + I_{\min}} . \qquad \text{Eq. (2)}$$

3.1.3 Image Patch

The camera was set up to be stationary for ease of capturing the images and analyzing them afterwards. A particular patch of the image was chosen to analyze the contrast, shown in Figure 6. The whole image contrast was not computed because the computation would take an exceedingly long time, given the size of the matrices and other factors. This particular chosen area is a part of the Singapore SingTel building wall where the wall is plated with white tiles and dark cement is in between the tiles. The distinctive colors of the tile and the cement make it easier to obtain more precise values of contrast.

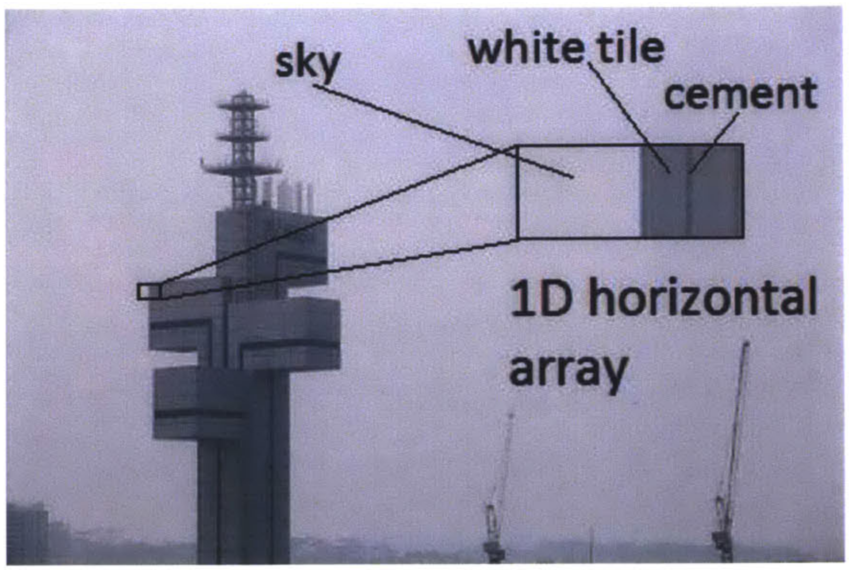

Figure 6. Diagram of the area used in analysis.

Since the sun's position changes throughout the day, some parts of the picture are in light while other parts are in shadow. At a given instant in time, every part of this chosen area is under the same illumination. As long as this area is under the same illumination, the contrast would be consistent and no normalization is needed. Suppose the area is under uniform illumination of magnitude A. Contrast is then defined by

$$Contrast = \frac{AI_{max} - AI_{min}}{AI_{max} + AI_{min}} \qquad \text{Eq (3)}$$

where A can be factored out, yielding

$$Contrast = \frac{A(I_{max} - I_{min})}{A(I_{max} + I_{min})} = \frac{I_{max} - I_{min}}{I_{max} + I_{min}}. \quad \text{Eq (4)}$$

This small area was a 1D array, shown by Figure 7 below. The number 1 denotes the part that contains I_{max}, the number 2 denotes the part that contains I_{min}. Figure 8 shows the profile of the luminosity amplitude of the 1D array. 1D array was chosen instead of an area or an average of many arrays because the images are very uniform, and during the calculations, the array profiles were smoothed out to eliminate noise. The smooth method is mentioned in the next section. The final contrast resulted from an area or the averages of many arrays did not have significant difference from that of the 1D array.

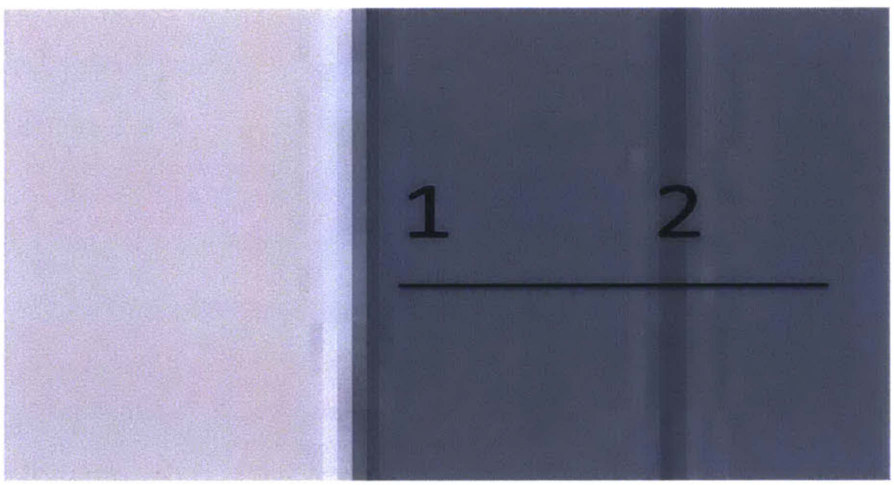

Figure 7. Example diagram of how the 1D array was taken.

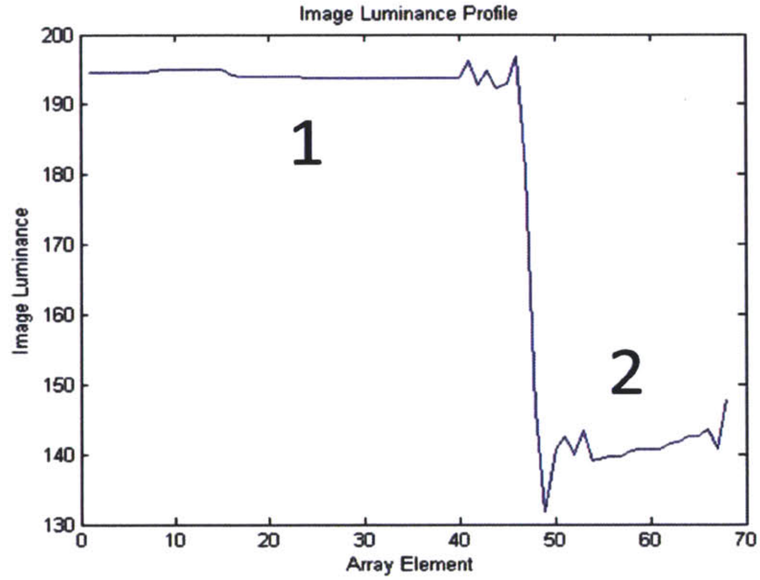

Figure 8. Example of a 1D array value profile, where 1 denotes the area of I_{max} and 2 denotes the area of I_{min}.

3.1.4 Contrast Calculations

Due to the distance between the camera and object of interest, and the limitation of camera resolution, a smoothing function was applied on the luminance profile to remove noise. The smoothing function smoothed the data by using a 5-point moving average. Five-point moving average was chosen because it was effective in mitigating noise while preserving important information. Then the maximum and minimum values were extracted to compute the contrast. Figure 9 shows the same array from Figure 8, after the smoothing function was applied.

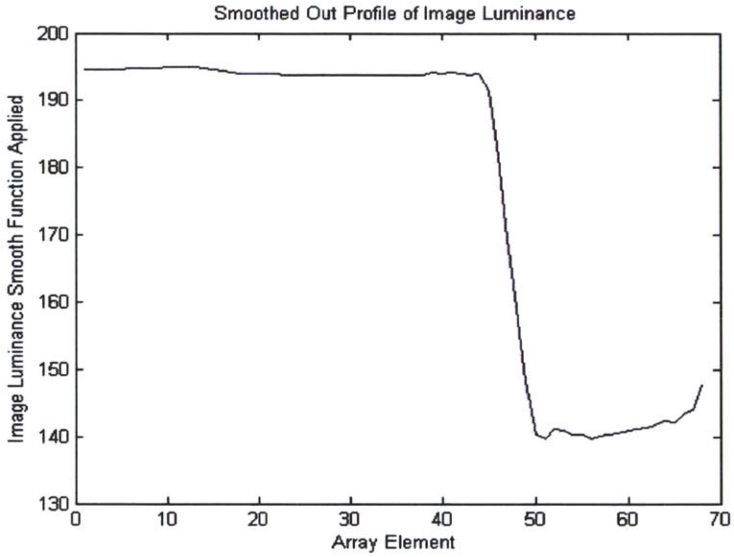

Figure 9. The smoothed out profile of the data in Figure 8.

3.1.5 Results and Analysis

Figure 10 below shows the computed contrast and PSI readings. Figure 11 shows the computed contrast fitted over the PSI readings to make the trend more visible. The contrast and PSI are on different scales, and the contrast graph was flipped and stretched to fit the PSI data. These manipulations are simply for the ease of visualization, and do not change the correlation between the two sets of data.

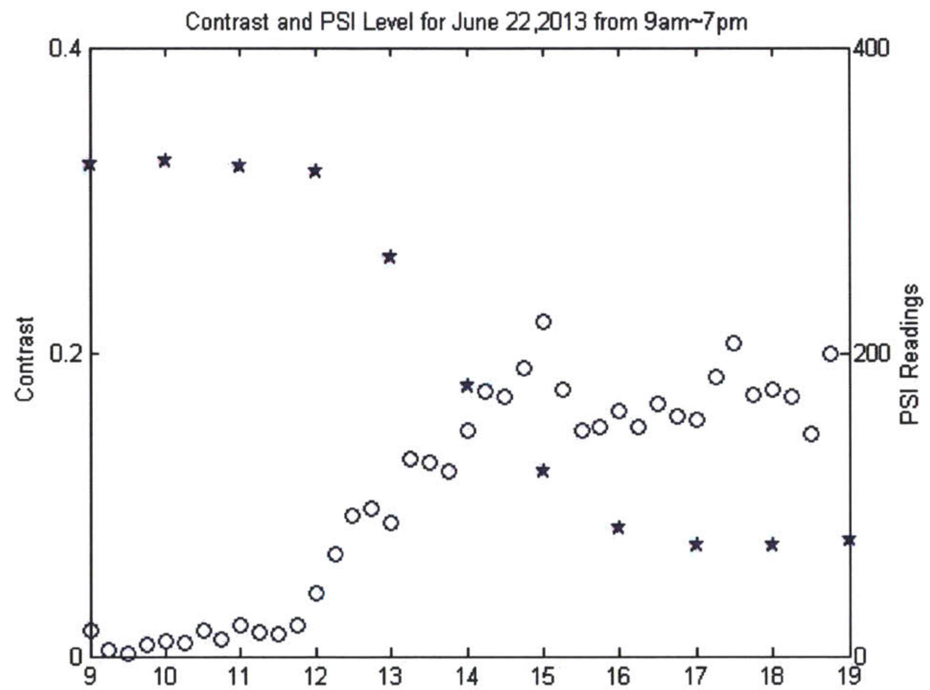

Figure 10. Contrast and PSI readings on June 22nd, 2014.

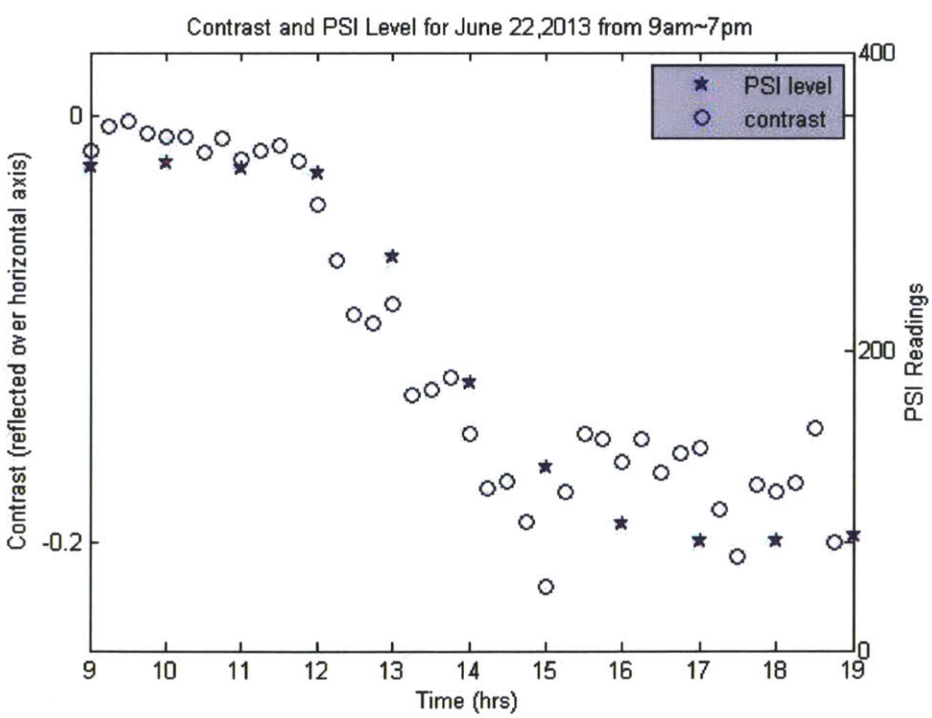

Figure 11. Contrast and PSI readings on June 22nd, 2014. Contrast is fitted over PSI readings.

3.2 Power Spectral Density Method

In this section, a general background of the power spectral density functions of the images is given. The power spectral density functions are analyzed and characterized in the following ways: maximum power, full width at half maximum, moments, and exponential fits.

3.2.1 Autocorrelation

Autocorrelation is the correlation of a signal with itself over some time t. It is often used to find repeating patterns in a signal over time in signal processing. Given a signal function $f(t)$, the autocorrelation is defined as

$$R(\tau) = (f(t) * \overline{f}(-t))(\tau) = \int_{-\infty}^{\infty} f(t)\overline{f}(t-\tau)dt, \qquad \text{Eq. 5}$$

where $\overline{f}$ is the complex conjugate of the original function, and τ is the time lag. The autocorrelation produces the similarity of the function and its time lagged version.

3.2.2 Power Spectral Density

The power spectral density gives information about the power of the signal for each frequency. Power spectral density is the Fourier transform of the autocorrelation of the real, stationary signal. Since the autocorrelation helps in identifying patterns in a signal in the time domain, the power spectral density examines these patterns in the frequency domain. The power spectral density is given by the Wierner–Khinchin theorem.

$$S(\omega) = \int_{-\infty}^{\infty} R(\tau)e^{-i\omega\tau}d\tau \qquad \text{Eq. 6}$$

where ω indicates frequency.

The power spectra density of an example image is shown in the figure below.

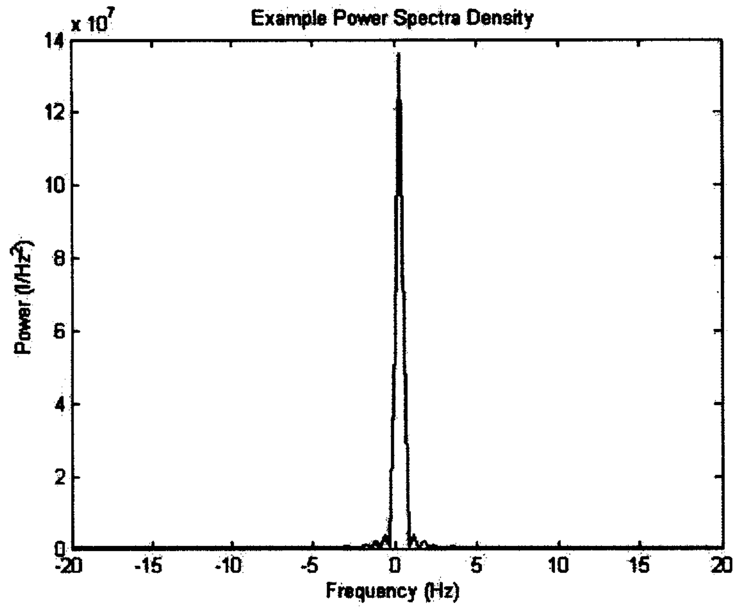

Figure 12. An example of a power spectra density function from an image in this experiment. Here, the I is used for the arbitrary intensity captured by the camera.

The Nyquist frequency is one half of the sampling rate of the signal processing. From the Nyquist criterion, the maximum recoverable frequency can be determined. The maximum frequency is half of the image size. In this test, the maximum frequency is 20 Hz.

3.2.3 Calculations and Results

Autocorrelation was performed on the same set of arrays as the contrast test. Autocorrelation was performed by using the MATLAB built-in function 'xcorr'. The result was then Fourier transformed to obtain the power spectral density. The result is quantified in different analysis methods in the following sections.

3.2.4 Maximum Power of the Power Spectra Density Function

In this method, the maximum power of the power spectrum of each array was extracted, and plotted against PSI.

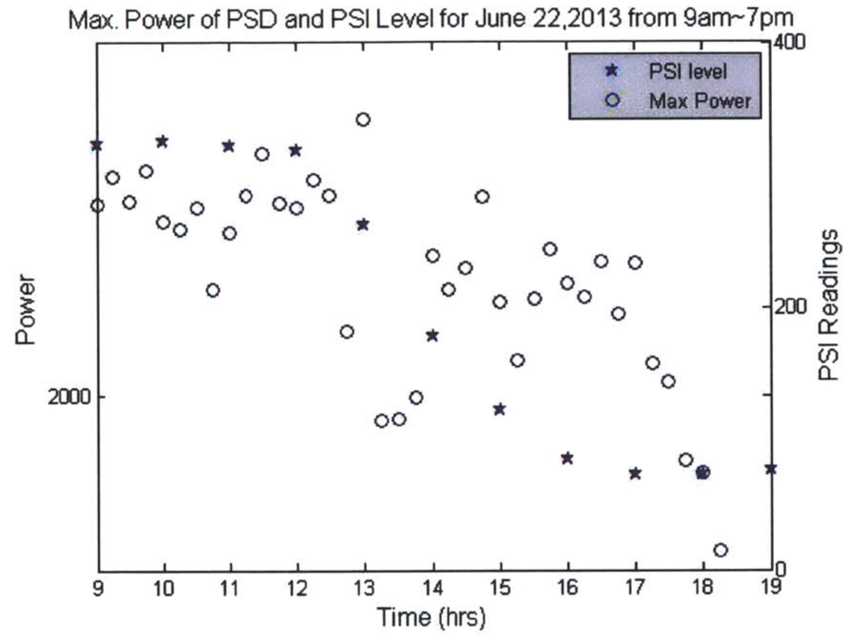

Figure 13. Maximum power in the power spectral density compared to PSI.

3.2.5 Full Width at Half Maximum

The full width of frequencies was measured at the half maximum of the frequency with the strongest power, shown in Figure 15. The full width-half maximum (FWHM) data was fitted to the PSI data points for the ease of visualization. Figure 14 shows an illustration of this method.

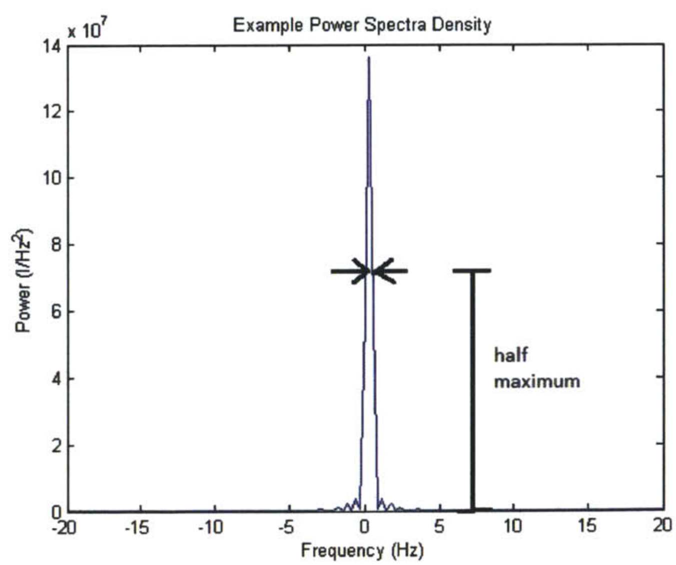

Figure 14. Illustration of the full width at half maximum method.

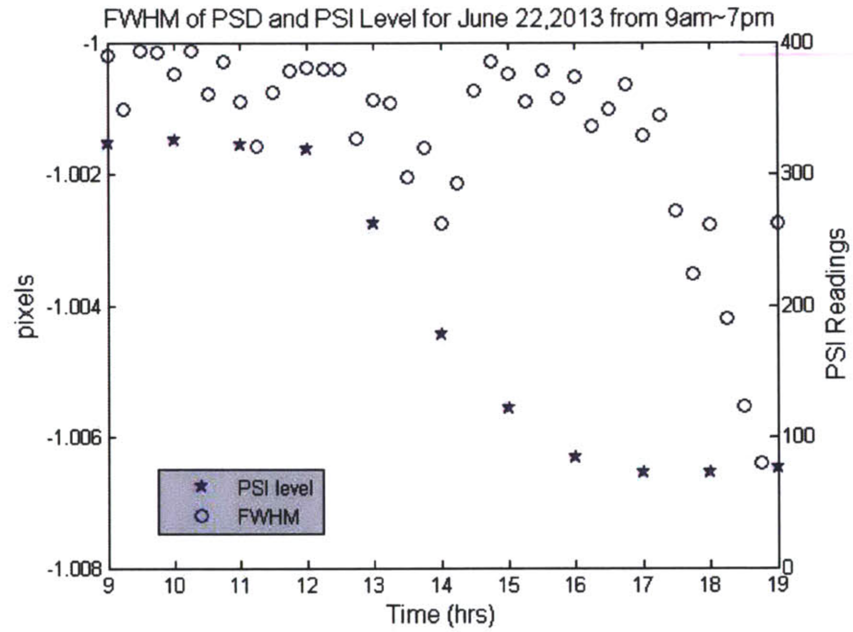

Figure 15. Full width at half maximum and PSI values.

3.2.6 Second and Third Moments of the Power Spectra Density

3.2.6.1 Moment

Moments are mathematical quantitative measurements of a set of data points. The n[th] moment of a signal can be computed by

$$\mu_n' = \int_{-\infty}^{\infty} (x-c)^n f(x)dx \qquad \text{Eq. 7}$$

Where f(x) is the function, c is the mean of the function. The mean, c can be computed by

$$c = \int x f(x)dx \quad . \qquad \text{Eq. 8}$$

3.2.6.2 Second Moment: Variance

The second moment, also call the central moment, is the variance of the signal. The second moment, variance, can be found by substituting n=2 into the general equation 7:

$$\mu_2' = \int_{-\infty}^{\infty} (x-c)^2 f(x)dx \quad . \qquad \text{Eq. 9}$$

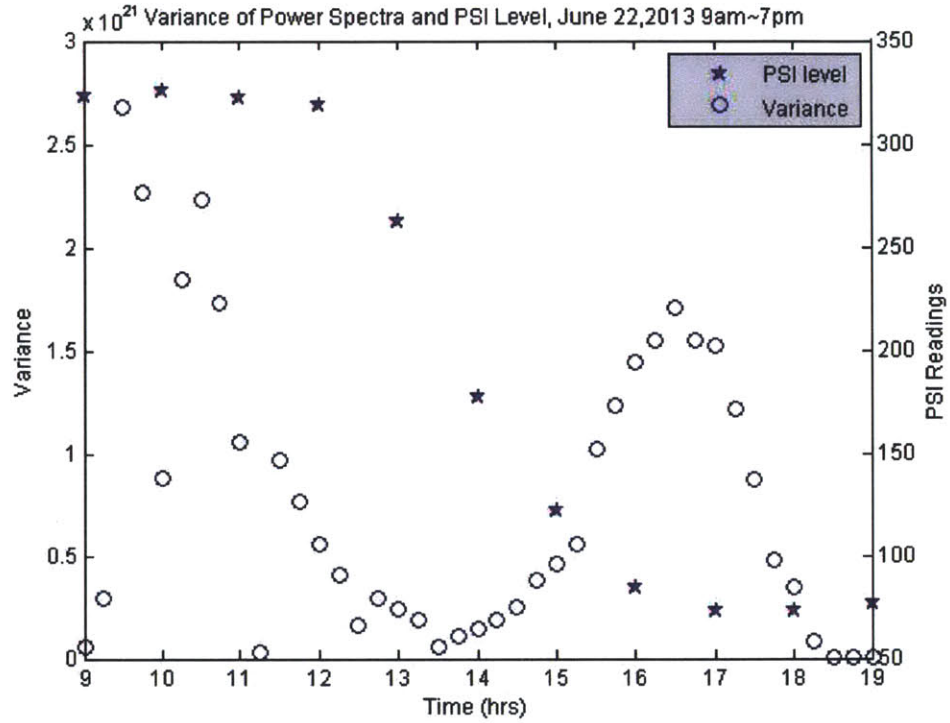

Figure 16. Plot of variance of the power spectrum and PSI level.

3.2.6.3 Third Moment: Skew

Skew is a measure of asymmetry of a function. A Gaussian would have a skew of zero, since it is symmetric. A negative skew indicates that the tail on the left side of the function is longer than that of the right side, and a positive skew would indicate the opposite.

Skew can be computed by substituting n=3 into Equation 7.

$$\mu_3' = \int_{-\infty}^{\infty} (x-c)^3 f(x)dx \qquad \text{Eq. 10}$$

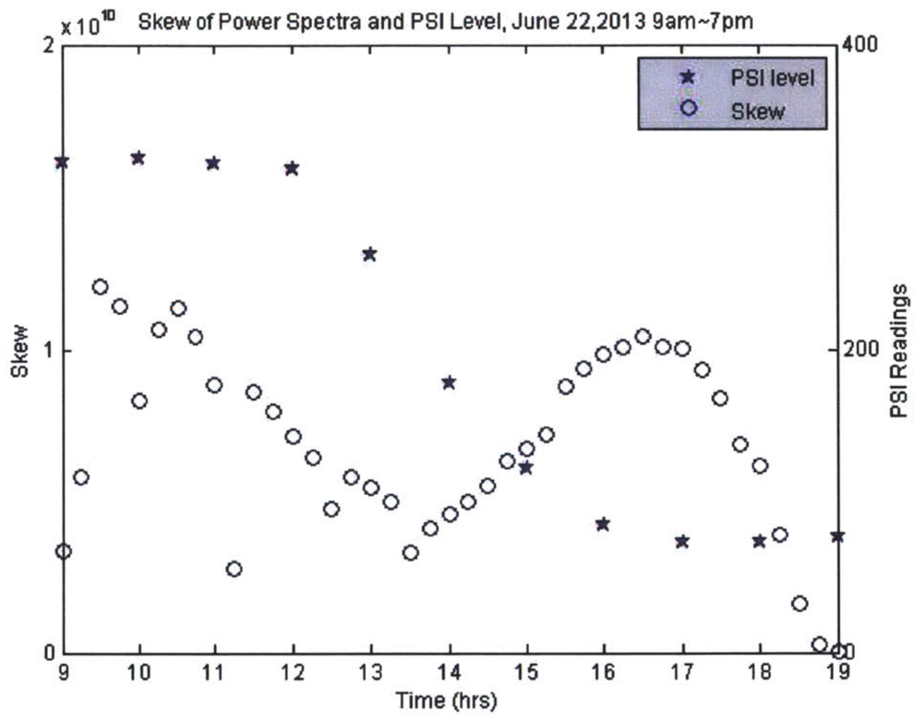

Figure 17. Graph of skew compared to PSI level.

3.2.7 Power of the Power Spectral Density

In this method, each power spectra density function was fitted to an exponential. Only the positive portion of the frequency spectrum was considered because the negative frequencies resulting from the equations do not represent physical quantities. The trend between the exponential and PSI was also investigated, shown in Figure 15.

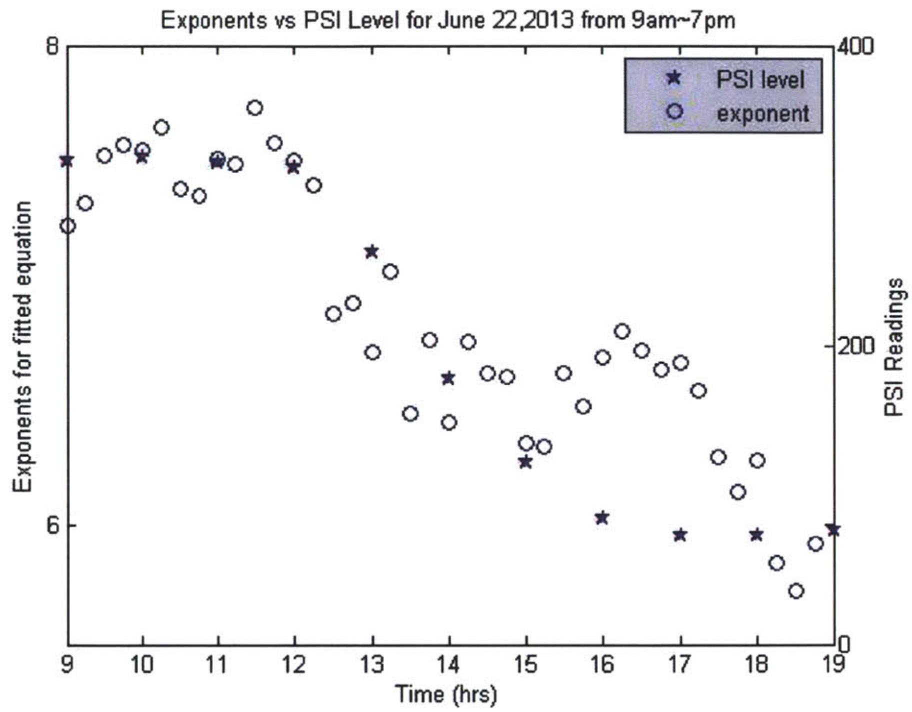

Figure 15. Exponent fit and PSI level.

4. Discussion and Future Work

The contrast method was shown to be the most correlated to the PSI readings. Among analysis that involved the power spectral density, the exponent fit showed to be the most correlated to the PSI readings. Images of near total darkness were not analyzed in this test because the lack of illumination would make many methods in this experiment difficult.

Some results from power spectral density methods showed correlation to the PSI readings for the time periods between 9am and 1pm, such as Figures 14, 15 and 17, but from 1pm to 7pm, these three figures all showed an increase and a decrease, whereas the PSI values showed a decreasing trend. The cause of this occurrence is unknown, but one speculation is that the PSI level after 1pm was comparatively lower than that in the morning, so particle turbulence could have had a more significant impact in those analyses.

In conclusion, the results from the analysis showed some correlation to the PSI levels. For future work, calibration and mapping of contrast values and exponential power of power spectral density to PSI values is a topic that can be investigated to allow for direct correspondence between the optical results and environmental readings.

Citations

Chew, Boon Ning, Chew Wai Chang, Santo Valentin Salinas, and Soo Chin Liew. 2009. *Remote Sensing Measurements of Aerosol Optical Thickness and Correlation with in-Situ Air Quality Parameters During a Biomass Burning Episode in Southeast Asia.*

Duparré, Angela, Josep Ferre-Borrull, Stefan Gliech, Gunther Notni, Jörg Steinert, and Jean M. Bennett. 2002. "Surface Characterization Techniques for Determining the Root-Mean-Square Roughness and Power Spectral Densities of Optical Components." *Applied Optics* 41 (1): 154–71. doi:10.1364/AO.41.000154.

"How Does Singapore Measure Haze Levels?" 2014. *Yahoo News Singapore*. Accessed May 6. https://sg.news.yahoo.com/how-does-singapore-measure-haze-levels--142610492.html.

HULBURT, E. O. 1941. "Optics of Atmospheric Haze." *Journal of the Optical Society of America* 31 (7): 467–72. doi:10.1364/JOSA.31.000467.

Kattawar, George W., and Gilbert N. Plass. 1968. "Radiance and Polarization of Multiple Scattered Light from Haze and Clouds." *Applied Optics* 7 (8): 1519. doi:10.1364/AO.7.001519.

Lin, L., M. Porkolab, E. M. Edlund, J. C. Rost, M. Greenwald, N. Tsujii, J. Candy, R. E. Waltz, and D. R. Mikkelsen. 2009. "Studies of Turbulence and Transport in Alcator C-Mod Ohmic Plasmas with Phase Contrast Imaging and Comparisons with Gyrokinetic Simulations." *Plasma Physics and Controlled Fusion* 51 (6): 065006. doi:10.1088/0741-3335/51/6/065006.

McCartney, E. J. 1976. "Optics of the Atmosphere: Scattering by Molecules and Particles." *New York, John Wiley and Sons, Inc., 1976. 421 P.* -1. http://adsabs.harvard.edu/abs/1976nyjw.book.....M.

"Meteorological Service Singapore." 2013. National Environment Agency. http://www.weather.gov.sg/wip/web/ASMC.

"NEA Spells Out How PSI Is Compiled." 2014. *Www.healthxchange.com.sg*. Accessed May 6. http://www.healthxchange.com.sg/News/Pages/nea-spells-psi-compiled.aspx.

"Singapore, Malaysia Hit by Haze." 2014. *BBC News*. Accessed May 6. http://www.bbc.com/news/world-asia-22935068.

US EPA, Region 1: New England. 2014. "Air Quality (Particulate Matter and Haze) | Topics | New England | US EPA". Overviews & Factsheets. Accessed May 11. http://www.epa.gov/region1/topics/pollutants/haze.html.

World Meterological Organization. 2013. "Singapore Affected by Severe Transboundary Smoke Haze". World Meteorological Organization.